UNIVERSITY OF LEEDS

White Rose
university consortium
Universities of Leeds, Sheffield & York

Geophysical Research Letters

Key Points:
- We simulated Amazon $\delta^{18}O_p$ and continental water recycling with and without forest cover
- The impact of forest removal on annual mean $\delta^{18}O_p$ is small relative to natural variability
- The large observed change in observed paleo-record $\delta^{18}O_p$ is unlikely due to substantial changes in the Amazon vegetation

Correspondence to:
K. C. Pattnayak,
k.c.pattnayak@leeds.ac.uk

Can We Detect Changes in Amazon Forest Structure Using Measurements of the Isotopic Composition of Precipitation?

K.C. Pattnayak[1,2] ID, J .C. Tindall[2] ID, R. J. W. Brienen[1] ID, J. Barichivich[3,4] ID, and E. Gloor[1] ID

[1]School of Geography, University of Leeds, Leeds, UK, [2]School of Earth and Environment, University of Leeds, Leeds, UK, [3]Instituto de Conservación, Biodiversidad y Territorio, Universidad Austral de Chile, Valdivia, Chile, [4]Center for Climate and Resilience Research, Santiago, Chile

Abstract Large-scale (>500 km) spatial gradients of precipitation oxygen isotope ratios ($\delta^{18}O_p$) hold information about the hydrological cycle. They result from the interplay between rainout and evapotranspiration along air-parcel paths, but these counteracting effects are difficult to disentangle, complicating quantification of the effect of land cover change on $\delta^{18}O_p$. We show that disentangling can qualitatively be achieved using climate model simulations with a land-derived precipitation tracer for tropical South America. We then either vary land cover as observed since 1870 or replace Amazon forests with bare land to determine the resulting signals. Our results indicate that effects of historically changing land cover on annual mean $\delta^{18}O$ isotope-ratio gradients are small and unlikely detectable, although there is a noticeable signal during the dry season. Furthermore, the effect of changes in water recycling on Amazon $\delta^{18}O_p$ in paleo-records may have been overestimated and need reinterpretation.

Plain Language Summary Deforestation causes reduction in precipitation downwind because trees act as pumps of water from soils to the atmosphere. This mechanism is primarily important during the dry season. How strong this effect is currently in the Amazon, given that approximately 20% of the forests have been cut, and how important it may be in the future if more forests are being destroyed is of great interest. One indicator of such changes is the east-west difference in heavy water isotope content of precipitation. While preferential rainout of the heavy isotope along air parcel trajectories enhances this difference, transpiration by forests decreases the difference. This is because forests inject water back into the atmosphere that is more enriched than the overlying water vapor. Records of this difference during the last ice age, in particular, have been interpreted in a previous study as providing information on continental recycling. We apply a land-derived water tagging approach in model simulations to investigate the effect of continental recycling on precipitation isotope content and to estimate this effect for varying land cover. We find that a 20% deforestation has only a small impact on precipitation isotope content. Even for a complete deforestation, in contrast to a previous interpretation, thus, only some of the isotopic signal observed during the ice age can be attributed to changes in continental recycling.

1. Introduction

Water droplets condensing from water vapor in air are enriched in the heavy water isotope $H_2^{18}O$ compared to the water vapor they condensed from (Dansgaard, 1964; Dansgaard et al., 1993). Accordingly, water vapor left behind in the atmosphere is slightly depleted in the heavy water isotope (isotopically slightly lighter). This fractionation process is weakly temperature dependent (Dansgaard, 1964) with fractionation decreasing with increasing temperature. In the absence of evaporation and transpiration, fractionation during condensation and condensate removal via precipitation will cause a gradual depletion of the heavy water isotope in water vapor of air parcels (so-called "Rayleigh distillation") travelling over the land. Put another way, and under the same conditions, spatiotemporal patterns in the precipitation isotope ratio $R \equiv H_2^{18}O/H_2^{16}O$ (mol/mol) contain information about the amount of condensation along an air-parcel's path and thus about the hydrological cycle, both today and in the past (Baker et al., 2016; Brienen et al., 2012; Salati et al., 1979; Thompson et al., 1995; van Breukelen et al., 2008; Wang et al., 2017; Wright et al., 2017). Air parcels moving into continents from the sea tend indeed to show an increasing heavy-isotope depletion signal the further into the continent they have travelled. This phenomenon is called "continental effect" (Dansgaard, 1964).
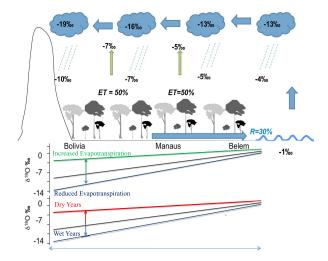
Figure 1. Simplified schematic of controls of Amazon basin precipitation δ18Op. Air masses enter the basin from the north-eastern Atlantic coast and then travel to the Andes where they are steered southward. Precipitation along this main air mass path causes an increasing depletion of the heavy water isotope in air mass water vapor, or, that is, a decrease in δ18Op with increasing distance from the northeastern Atlantic coast ("Continental effect"). Transpiration reinserts previously rained out heavy isotope water vapor into overlying air and thus counteracts the δ18Op signal caused by precipitation. The net resulting East-West gradient thus reflects the difference between these two controls. The isotope values in the figure are fictional and serve only illustrative purposes.

The signal is a decrease in R or equivalently in $\delta^{18}O$ $(^0/00) \equiv (R/R_{st} -1)*10^3$ where $R_{st} = 2.0052 \times 10^{-3}$ (mol/mol) is the abundance ratio of Vienna Standard Mean Ocean Water (Baertschi, 1976; Figure 1) with increasing distance from the coast.

While precipitation causes water vapor of air travelling over land to gradually become isotopically lighter, only a fraction of precipitated water will run off via rivers, and the rest will eventually be reinserted into the airstream via evaporation and plant transpiration. If precipitated water is reinserted by transpiration, this will counteract the depletion in air masses due to condensation and precipitation because plant transpiration is a nonfractionating process (Barnes & Allison, 1988; Washburn & Smith, 1934; Figure 1). Large-scale patterns of precipitation isotope ratios as well as changes of these patterns over time thus contain not only information about precipitation but also "recycled" water from plant transpiration. These in turn are expected to depend on vegetation type (forest vs. grassland) particularly during the dry season. This is because near-surface compartments of the soil dry more rapidly compared to deeper compartments during the dry season, and thus, shallow-rooted grasslands will recycle less water than deep-rooted forests (Zhang et al., 2001).

The relative importance of the two counteracting "controls" on precipitation isotope ratios, precipitation, and transpiration is of interest on various timescales. It is, for example, important for the interpretation of paleo-isotope records obtained from speleothems (Wang et al., 2017), which aim to resolve whether climate in the Amazon was drier or wetter during the Last Glacial Maximum (LGM) compared to today. The Amazon offers itself for analysis of its hydrological cycle with isotopes because of the large distance air travels over the basin. Air enters the basin from the tropical Atlantic via the trade winds and then travels toward the Andes where the air stream bends southward and flows back toward the Atlantic in southeastern direction. This main air path varies only weakly between wet and dry season. Wang et al. (2017) reported a very small Amazon east-west $\delta^{18}O_p$ gradient in the "early to mid-Holocene" but a much larger gradient of up to $-2.8^0/00/1,000$ km during the LGM. They attribute the larger isotopic gradient at LGM to a strong reduction in water recycling caused by much reduced area covered by rainforests (see also Pierrehumbert, 1999; Thompson et al., 2000). However, to our knowledge the magnitude of the effect of forest area reduction on water recycling and water isotopes has not yet been estimated jointly using realistic models. Spatial patterns in $\delta^{18}O_p$ may also contain interesting information in regions like the Amazon today where both global warming and the rapid ongoing large-scale transformation of the land surface of both Cerrado and humid forest biomes are likely to impact the hydrological cycle (Brienen et al., 2012; Dias et al., 2015; Spera

et al., 2016). While future climate model predictions of the tropical South American hydrological cycle vary, they tend to suggest that greenhouse warming will lead to drier conditions. The lesser rainout would lead to a decrease of the Amazon-wide east-west difference in $\delta^{18}O_p$. In contrast, lesser continental recycling would increase it. Therefore, disentangling the effect of precipitation versus transpiration on $\delta^{18}O_p$ is not straight-forward and proper attribution of observed $\delta^{18}O_p$ gradients difficult.

Here we use a General Circulation Model (GCM), to relate $\delta^{18}O_p$ signals over South America to the amount of precipitation and continental recycling. We also investigate the signal in precipitation oxygen isotope ratios, precipitation amount, and continental recycling that would theoretically result from complete removal of Amazon rainforests, as well as from historically changing land cover and greenhouse gases. The novel element of the study is the simultaneous quantification of the effects of changes in forest cover on both water recycling and precipitation isotope signals. The results have implications for the interpretation of $\delta^{18}O_p$ spatial gradients both over the past 50 years resulting from land use change and the LGM.

2. Data and Methodology

2.1. Isotope-Enabled Climate Model HadAM3

To simulate climate, including water isotope cycling, we use the atmospheric component of the isotope enabled version of Hadley Centre Climate model (HadAM3; Pope et al., 2000) with prescribed observed sea surface temperatures. Several researchers have evaluated the skill of the fully coupled version of HadCM3 to model the present South American climate (Cabré et al., 2016; Chou et al., 2011; Reboita et al., 2014; Tindall et al., 2009) and found that the model performs well. How isotopes are represented in the model has been described in detail in Tindall et al. (2009). Processes on land are treated in a simple way with no fractionation during evaporation from vegetation covered land, during sublimation from ice, exchange of water between adjacent soil layers and evaporation from soils. Thus, we assume that most of evapotranspiration is via transpiration (Jasechko et al., 2013; Schlesinger & Jasechko, 2014), neglecting fractionation during evaporation from open water, soils (Mathieu & Bariac, 1996; Melayah et al., 1996), and water intercepted by the canopy (Gat & Matsui, 1991).

The skill of the isotope component has been evaluated for several regions with positive results. Tindall et al. (2009) showed that simulated $\delta^{18}O_p$ compares well with observations. Sime et al. (2008) found that the geographical pattern of modeled present-day Antarctic $\delta^{18}O_p$ agrees well with 20th century $\delta^{18}O$ Antarctic surface snow (Masson-Delmotte et al., 2008). We have further evaluated the skills of the HadAM3 forced by observed sea surface for South America with results being discussed in section 2.3.

Although the skills of the model for contemporary times are high, neglecting fractionation during evaporation from water surfaces, soils, and canopy-intercepted water is a limitation of this study. As the contribution of evaporation compared to transpiration may increase with forest removal, neglecting these effects may cause underestimation of the change in water vapor isotopic depletion along air parcel paths caused by forest removal (Haese et al., 2013; Risi et al., 2016).

2.2. Land-Derived Precipitation Fraction Tracer

For this work, two new hydrological tracers have been incorporated into HadAM3 motivated by the concepts introduced by van der Ent et al. (2010). One of the new tracers will "tag" water that is evaporated from the ocean, while the other will tag water that is evaporated or transpired from land (also termed recycled water). Although water tagging has been included in other isotope-enabled GCMs (Eckstein et al., 2018; Jouzel et al., 2013; Koster et al., 1986; Numaguti, 1999; Risi et al., 2010, 2013; Yoshimura et al., 2004), this is the first time that this feature has been used operationally in HadCM3. This water tagging will allow us to investigate whether the recycled proportion of precipitation changes under different scenarios and relate this to modeled $\delta^{18}O_p$.

2.3. Climate Model Simulations

We investigate the hydrological cycle over South America and how it is reflected in $\delta^{18}O_p$ with four factorial simulations (Table S1 in the supporting information). First, there is a control simulation (CONTROL) that is forced with sea surface temperatures (SST's) and sea ice cover from 1870 to 2016 from the Hadley Centre
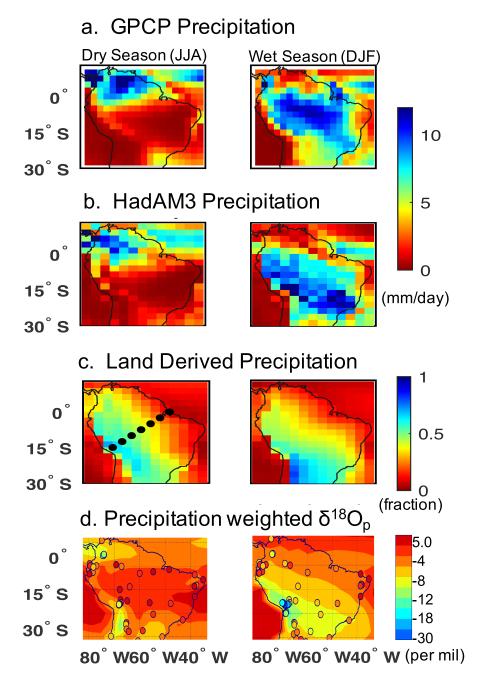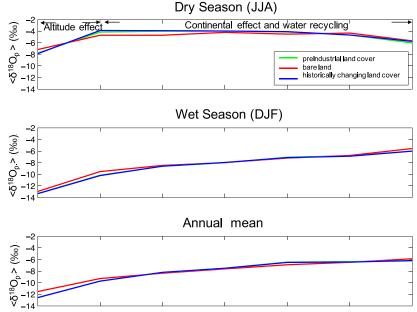
Figure 2. Total precipitation, land-precipitation (fraction), and precipitation δ18O predicted for preindustrial land cover and atmospheric greenhouse gas levels (1985–2014 means.) Left column: dry season (June–August); right column: wet season (December–February); top two rows: mean precipitation (mm/day); top row: GPCP precipitation; second row from the top: HadAM3 simulated precipitation; third row from the top: land-derived precipitation (fraction); bottom row: δ18Op (0/00). The black dots on the third row from the top have been used to present the gradient of δ18Op in the later part of the study (Figure S4).

Global Sea Ice and Sea Surface Temperature (HadISST) data sets (Rayner et al., 2003); prescribed with constant CO_2 and CH_4 levels of 280 and 760 ppbv, respectively; and initialized with sea water and soil moistures $\delta^{18}O$ of 0‰ and ice sheet $\delta^{18}O_p$ of −40‰ (Tindall et al., 2009).

The three additional experiments are (1) NOVEG (as CONTROL but with vegetation replaced by bare soil), (2) OBS_VEG (as CONTROL but with time-varying vegetation according to observations), and (3)

Figure 3. Precipitation δ18O northeast southwest along the transect across the Amazon basin indicated in Figure 2c (dotted line) during the dry season (top panel), wet season (middle panel), and the whole year (bottom panel) for the preindustrial land cover and atmospheric greenhouse gas level simulation.

OBS_GHG_VEG (as CONTROL but with both vegetation and greenhouse gases varying according to observations. Time-varying vegetation cover from 1870 to 2016 is based on the reconstructions of Meiyappan and Jain (2012). For the NOVEG experiment broad leaf trees, the primary vegetation type of the Amazon humid forests was replaced by bare land (Figures S1 and S2). This corresponds to complete clear-cutting of the rain forests. For simulations with changing greenhouse gas levels, we prescribed CO_2 and CH_4 concentrations using reconstructions from ice cores up to 1959 and in situ measurements thereafter. These two gases account for ~90% of anthropogenically caused radiative forcing. Comparisons of model-simulated precipitation with the Global Precipitation Climatology Project (GPCP; Adler et al., 2003) show that the model reproduces the observed precipitation seasonal cycle for tropical South America (Figures 2a and 2b) with maximum precipitation over Venezuela and low precipitation over the Amazon during June–August (Amazon "dry season") and high precipitation over the Amazon during December–February (Amazon "wet season"). Model-predicted wet season precipitation is somewhat larger in the southwest of the basin and lower in Central Amazon compared to observations. Spatial patterns and seasonality of precipitation-weighted precipitation isotope ratio records from the Global Network of Isotopes in Precipitation (GNIP; IAEA/WMO, 2006) are also well captured by the model (Figure 2d). Specifically, during the dry season, isotope signals are uniform across the Amazon, while during the wet season there is a N-E to S-W gradient both in the model predictions and observations. Similarly, main patterns across all of South America are quite well captured. To be more quantitative, we used an F test to test whether the variance of the difference between observations and simulations is less than the variance of the observations for South American sites, both for the wet and the dry season. The test result is highly significant for both wet and dry seasons with $p < 0.01$ and $p < 0.002$, with variance ratios of 0.48 and 0.40, respectively. The RMS difference between simulations and observations is 3.1‰ and 2.7‰ for DJF and JJA, with observation's standard deviation of 6.5‰ and 5.7‰, respectively.

Seasonality is mostly well captured with exception of a Colombian site close to the Caribbean Sea and two Western Andean Ecuadorian sites. For two thirds of the sites time correlations of monthly means with observations were significant at 95% level with correlation coefficients >0.6. Our model captures also the seasonality of evapotranspiration well compared with the data-based estimates of Maeda et al. (2017; Figure S3), specifically that evapotranspiration starts before the onset of the wet season.
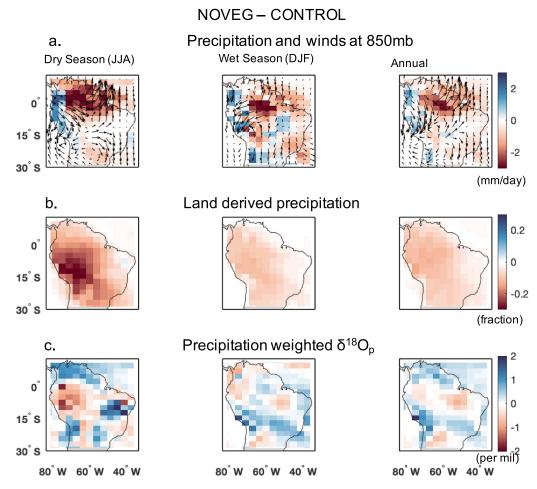
Figure 4. Mean difference in precipitation (mm/day) and wind at 850 hPa (top row), land-derived precipitation (midrow), δ18Op (bottom row) between deforestation simulation (NOVEG, Table S1), and fixed preindustrial land cover simulation (CONTROL) for the period from 1985 to 2014. Left column: difference during dry season (June–August); middle column: during wet season (December–226 February) and during the entire year.

3. Results

Figure 2 shows the precipitation amount, the fraction of precipitation that is recycled, and the $\delta^{18}O_p$ of precipitation for the CONTROL experiment. Wet season precipitation (December–February; Figure 2a) increases from the Atlantic coast to the Andes along the transect shown in Figure 3. Dry season (June–August) precipitation amount peaks in the northwest of the basin north of the equator and otherwise is low. In contrast to precipitation amount, the recycled precipitation fraction changes little between seasons although there is a shift of the maximum from approximately 15°S in the Western Amazon during the dry season to 25°S to 30°S along the Eastern foothills of the Andes to the South of the Amazon during the wet season (Figure 2b). Spatial patterns and seasonality are similar to previous studies (Staal et al., 2018; Zemp et al., 2017), and magnitude of Amazon basin annual mean land-derived precipitation fraction of 38% is within the range of 10 previous estimates as summarized in Staal et al. (2018).

As expected, HadCM3 predicts a steady decrease in $\delta^{18}O_p$ along the path of the main airstream during the wet season. However, during the dry season, there is no noticeable decrease in $\delta^{18}O_p$ over most of the basin (Figures 2 and 3). The wet season east-west difference across the basin (along the dotted line on Figure 2c) is ~4⁰/00 with a further ~4⁰/00 depletion from 12.5°S to 15°S. This latter decrease is caused in the model by cooling of air when ascending the slopes of the Andes, known as "altitude effect," (Dansgaard, 1964). This suggests that during the wet season, intense precipitation along the airstream and associated Rayleigh distillation is the main control of $\delta^{18}O_p$. In contrast during the dry season, the spatial pattern of $\delta^{18}O_p$ is not
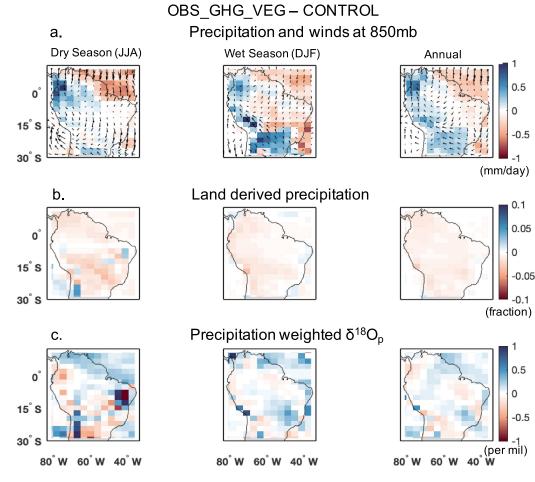
Figure 5. Mean difference in precipitation (mm/day; and wind at 850 hPa top row), land-derived precipitation fraction (midrow), and δ18Op (bottom row) between historically changing land surface cover simulation (OBS_GHG_VEG, Table S1) and fixed preindustrial land cover simulation (CONTROL) for the period from 1985 to 2014. Left column: difference for dry season (June–August); middle column: for wet season (December–February); and right column: during the entire year.

consistent with the spatial pattern of precipitation, suggesting that across large parts of the Amazon basin part with low precipitation), the $\delta^{18}O_p$ signal is not due to the classical "amount effect" or Rayleigh distillation. Instead, the $\delta^{18}O_p$ signal is consistent with increasing continental recycling along the transect in Figure 2c. The differences in land-derived precipitation fraction between wet and dry season are small, and so continental recycling alone cannot be the cause of differences in $\delta^{18}O_p$ gradients between seasons.

To understand the effect of land-surface changes on water isotopes, it is instructive to consider the picture resulting for the most drastic land surface cover change scenario where we replace all humid forests by bare land (Table S1 and Figure S1). Replacement of tropical humid forests leads to an increase in 850-mb wind divergence over the northern and central part of tropical South America during the dry season, and along an approximately 1,000-km-wide zone along the northeastern Atlantic coast and Central Amazonia during the wet season (Figures S4b and 4a). These changes cause substantial decreases in precipitation in Central and Northern Amazonia and in the River Plata catchment during the dry season, as well as in Central Amazonia during the wet season (Figure 4). This result is consistent with the well-known studies of Nobre et al. (1991), Shukla et al. (1990), and follow-up studies like Costa and Foley (1997). Figure 4a shows changes in precipitation and winds between the NOVEG experiment and the CONTROL experiment. Although precipitation is larger over the Andes, most of tropical South America shows a strong decrease in precipitation.

In the NOVEG simulation the proportion of recycled precipitation has drastically reduced as expected (Figure 4b). However, it is the reduction in recycled precipitation over the dry season that is most

remarkable. Here the recycled precipitation fraction decreases by up to ~60% in southwest direction from the northeastern Atlantic coast and south of the equator. In contrast, during the wet season, land-derived precipitation fraction changes much less (less than 20%).

Figure 4c shows the change in $\delta^{18}O_p$ between the NOVEG and the CONTROL experiment. As expected, the wet season shows a weaker decrease of $\delta^{18}O_p$ along the main air stream (as compared to CONTROL), which can be related to the reduction in rainfall seen in Figure 4a. In the dry season, however, there is a substantial region over the west of South America, which shows reduced precipitation but also reduced $\delta^{18}O_p$, which appears at odds with the classical amount-effect interpretation. In this region the fraction of recycled precipitation shows the most substantial decrease (Figure 4b). Theoretically, this reduction in recycled precipitation would shift the distillation slope further toward the classical Rayleigh distillation shown in Figure 1 and would be expected to lead to a reduction in $\delta^{18}O_p$ along the airstream. Therefore, the depletion in $\delta^{18}O_p$ seen in the deforestation scenario is consistent with the substantial reduction in recycled water.

Overall, for full forest-cover-removal-induced signals in $\delta^{18}O_p$, changes in rainfall are the primary control during the wet season, while reductions in land-derived precipitation may play a role during the dry season. However, the simulations presented in this paper do not allow to quantify the contribution of land-derived precipitation fraction changes to $\delta^{18}O_p$ changes. Additional tracers for land-derived precipitation isotopologues would be necessary to quantify this contribution (Risi et al., 2010, 2013).

While the simulation for the extreme NOVEG scenario shows how accounting for continental recycling can explain modeled $\delta^{18}O_p$, such a scenario does not reflect the actual land use change in tropical South America. Actual changes are much less extreme and have resulted in deforestation of approximately 20% (Figures S1 and S2). The difference of $\delta^{18}O_p$ between the historical land-cover change simulation and fixed preindustrial land-cover simulation can be understood in a similar way as the bare land simulation but signals are much smaller (Figure 5). During the dry season, there is similarly a precipitation decrease in the north-east in a region parallel to the northeastern Atlantic coast. During the wet season, the precipitation decreases in most of tropical South America, while there is an increase along the Andes and the air outflow region of the Amazon (region south of ~18°S).

In comparison to the NOVEG simulations the contrast between dry and wet season for the land-derived precipitation fraction is much weaker. The most notable signature is a decrease during the dry season in the southern half of the Amazon and further to the south of the Amazon—including the Amazon air outflow region (directed from Bolivia toward the Sao Paulo region).

$\delta^{18}O_p$ patterns are again similar with enrichment during the dry season along a zone parallel to the northeastern Atlantic coast reflecting a decrease in precipitation and a depletion in Western Amazonia and most of southern parts of tropical South America (with the exception primarily of the Andes) reflecting both changes in precipitation and likely also water recycling; during the wet season, there is enrichment where precipitation decreased and vice versa. Annual mean signals mirror primarily changes of precipitation during the wet season and are quite small (Figure 5).

4. Discussion and Conclusions

Oxygen isotopes in precipitation ($\delta^{18}O_p$) can potentially give us information about changes in the hydrological cycle over large areas and a range of timescales as recorded in climate archives. We investigate here this information and its controls for tropical South America using factorial simulations with the isotope enabled atmospheric component of HadCM3. We vary land cover using an extreme bare ground scenario with all Amazon forests replaced and a more realistic scenario where we change land cover and atmospheric greenhouse gas concentrations over time according to reconstructions/observations (Meiyappan & Jain, 2012). We neglect fractionation-effects caused by evaporation from open water surfaces, soil, and canopy-intercepted water.

We find the following. During the wet season, the amount of recycled precipitation changes little even if there is a substantial land cover change. Thus, during the wet season, the difference of spatial patterns of $\delta^{18}O_p$ between simulations with different land cover mirror primarily the induced precipitation amount differences via changes in Rayleigh distillation. In contrast, during the dry season, the amount of recycled water decreases markedly when forests are removed, and this decrease may contribute substantially to a lower

$\delta^{18}O_p$ in the central-western part of the Amazon. Thus, to detect the effect of vegetation cover changes on evapotranspiration, it is best to measure dry season $\delta^{18}O_p$ because signals are largest. We find similar patterns/controls for the difference between simulations with historical land cover changes compared to simulations without land-cover change, but the differences in signals are much smaller.

In more detail our simulations suggest that the large land cover changes in the Amazon, which occurred predominantly since the 1970s and have led to a decrease of approximately 20% of the Amazonian forests, cause only a small land-derived precipitation change (up to maximally a 4% decrease during the dry season and less during the wet season). Precipitation decrease extends over all of Eastern and Central Amazonia but is also quite small (up to ~0.4 mm/day or ~7 cm in total during the wet season). Similar to the extreme bare land scenario annual-mean precipitation-weighted $\delta^{18}O_p$ changes caused by historically observed deforestation are the result of the changes in wet season precipitation. The signals are small (up to ± 0.2‰) and unlikely to be detectable given natural variability of $\delta^{18}O_p$. While on its own this result is a bit disappointing, it may be that addition of precipitation δD measurements will improve detectability of hydrological cycle changes (Henderson-Sellers et al., 2004). It permits to calculate deuterium excess ($\delta D-8*\delta^{18}O_p$), which provides information on water recycling from open water surfaces on land (Aemisegger et al., 2014; Risi et al., 2016).

Our results are also relevant for recent paleo-climate studies like Wang et al. (2017), who suggested that the small east-west difference of speleothem-derived $\delta^{18}O_p$ during the early and mid-Holocene, but large difference (~3‰) during the LGM, can be explained by changes in vegetation cover. Our results suggest that land cover changes can only account for a small change in east-west $\delta^{18}O_p$ differences; thus, interpretation of these records may need some further thought.

References

Adler, R. F., Huffman, G. J., Chang, A., Ferraro, R., Xie, P. P., Janowiak, J., et al. (2003). The Version-2 Global Precipitation Climatology Project (GPCP) Monthly Precipitation Analysis (1979–Present). *Journal of Hydrometeorology*, *4*(6), 1147–1167. https://doi.org/10.1175/1525-7541(2003)004<1147:TVGPCP>2.0.CO;2

Aemisegger, F., Pfahl, S., Sodemann, H., Lehner, I., Seneviratne, S. I., & Wernli, H. (2014). Deuterium excess as a proxy for continental moisture recycling and plant transpiration. *Atmospheric Chemistry and Physics*, *14*(8), 4029–4054. https://doi.org/10.5194/acp-14-4029-2014

Baertschi, P. (1976). Absolute18O content of standard mean ocean water. *Earth and Planetary Science Letters*, *31*(3), 341–344. https://doi.org/10.1016/0012-821X(76)90115-1

Baker, J. C. A., Gloor, M., Spracklen, D. V., Arnold, S. R., Tindall, J. C., Clerici, S. J., et al. (2016). What drives interannual variation in tree ring oxygen isotopes in the Amazon? *Geophysical Research Letters*, *43*, 11,831–11,840. https://doi.org/10.1002/2016GL071507

Barnes, C. J., & Allison, G. B. (1988). Tracing of water movement in the unsaturated zone using stable isotopes of hydrogen and oxygen. *Journal of Hydrology*, *100*(1-3), 143–176. https://doi.org/10.1016/0022-1694(88)90184-9

Brienen, R. J., Helle, G., Pons, T. L., Guyot, J. L., & Gloor, M. (2012). Oxygen isotopes in tree rings are a good proxy for Amazon precipitation and El Nino-Southern Oscillation variability. *Proceedings of the National Academy of Sciences of the United States of America*, *109*(42), 16,957–16,962. https://doi.org/10.1073/pnas.1205977109

Cabré, M. F., Solman, S., & Núñez, M. (2016). Regional climate change scenarios over southern South America for future climate (2080-2099) using the MM5 Model. Mean, interannual variability and uncertainties. *Atmosfera*, *29*(1), 35–60. https://doi.org/10.20937/ATM.2016.29.01.04

Chou, S. C., Marengo, J. A., Lyra, A. A., Sueiro, G., Pesquero, J. F., Alves, L. M., et al. (2011). Downscaling of South America present climate driven by 4-member HadCM3 runs. *Climate Dynamics*, *38*(3-4), 635–653. https://doi.org/10.1007/s00382-011-1002-8

Costa, M. H., & Foley, J. A. (1997). Water balance of the Amazon Basin: Dependence on vegetation cover and canopy conductance. *Journal of Geophysical Research*, *102*(D20), 23,973–23,989. https://doi.org/10.1029/97JD01865

Dansgaard, W. (1964). Stable isotopes in precipitation. *Tellus*, *16*(4), 436–468. https://doi.org/10.1111/j.2153-3490.1964.tb00181.x

Dansgaard, W., Johnsen, S. J., Clausen, H. B., Dahl-Jensen, D., Gundestrup, N. S., Hammer, C. U., et al. (1993). Evidence for general instability of past climate from a 250-kyr ice-core record. *Nature*, *364*(6434), 218–220. https://doi.org/10.1038/364218a0

Dias, L. C. P., Macedo, M. N., Costa, M. H., Coe, M. T., & Neill, C. (2015). Effects of land cover change on evapotranspiration and streamflow of small catchments in the Upper Xingu River Basin, Central Brazil. *Journal of Hydrology: Regional Studies*, *4*, 108–122. https://doi.org/10.1016/j.ejrh.2015.05.010

Eckstein, J., Ruhnke, R., Pfahl, S., Christner, E., Diekmann, C., Dyroff, C., et al. (2018). From climatological to small-scale applications: Simulating water isotopologues with ICON-ART-Iso (version 2.3). *Geoscientific Model Development*, *11*(12), 5113–5133. https://doi.org/10.5194/gmd-11-5113-2018

Gat, J. R., & Matsui, E. (1991). Atmospheric water balance in the Amazon basin: An isotopic evapotranspiration model. *Journal of Geophysical Research*, *96*(D7), 13,179–13,188. https://doi.org/10.1029/91jd00054

Haese, B., Werner, M., & Lohmann, G. (2013). Stable water isotopes in the coupled atmosphere-land surface model ECHAM5-JSBACH. *Geoscientific Model Development*, *6*(5), 1463–1480. https://doi.org/10.5194/gmd-6-1463-2013

Henderson-Sellers, A., McGuffie, K., Noone, D., & Irannejad, P. (2004). Using stable water isotopes to evaluate basin-scale simulations of surface water budgets. *Journal of Hydrometeorology*, *5*(5), 805–822. https://doi.org/10.1175/1525-7541(2004)005<0805:USWITE>2.0.CO;2

IAEA/WMO (2006). Global network of isotopes in precipitation. The GNIP Database.

Jasechko, S., Sharp, Z. D., Gibson, J. J., Birks, S. J., Yi, Y., & Fawcett, P. J. (2013). Terrestrial water fluxes dominated by transpiration. *Nature*, *496*(7445), 347–350. https://doi.org/10.1038/nature11983

Jouzel, J., Delaygue, G., Landais, A., Masson-Delmotte, V., Risi, C., & Vimeux, F. (2013). Water isotopes as tools to document oceanic sources of precipitation. *Water Resources Research*, *49*, 7469–7486. https://doi.org/10.1002/2013WR013508

Koster, R., Jouzel, J., Suozzo, R., Russell, G., Broecker, W., Rind, D., & Eagleson, P. (1986). Global sources of local precipitation as determined by the Nasa/Giss GCM. *Geophysical Research Letters*, *13*(2), 121–124. https://doi.org/10.1029/GL013i002p00121

Maeda, E. E., Ma, X., Wagner, F. H., Kim, H., Oki, T., Eamus, D., & Huete, A. (2017). Evapotranspiration seasonality across the Amazon Basin. *Earth System Dynamics*, *8*(2), 439–454. https://doi.org/10.5194/esd-8-439-2017

Masson-Delmotte, V., Hou, S., Ekaykin, A., Jouzel, J., Aristarain, A., Bernardo, R. T., et al. (2008). A review of Antarctic surface snow isotopic composition: Observations, atmospheric circulation, and isotopic modeling*. *Journal of Climate*, *21*(13), 3359–3387. https://doi.org/10.1175/2007JCLI2139.1

Mathieu, R., & Bariac, T. (1996). A numerical model for the simulation of stable isotope profiles in drying soils. *Journal of Geophysical Research*, *101*(D7), 12,685–12,696. https://doi.org/10.1029/96jd00223

Meiyappan, P., & Jain, A. K. (2012). Three distinct global estimates of historical land-cover change and land-use conversions for over 200 years. *Frontiers of Earth Science*, *6*(2), 122–139. https://doi.org/10.1007/s11707-012-0314-2

Melayah, A., Bruckler, L., & Bariac, T. (1996). Modeling the transport of water stable isotopes in unsaturated soils under natural conditions: 2. Comparison with field experiments. *Water Resources Research*, *32*(7), 2055–2065. https://doi.org/10.1029/96wr00673

Nobre, C. A., Sellers, P. J., & Shukla, J. (1991). Amazonian deforestation and regional climate change. *Journal of Climate*, *4*(10), 957–988. https://doi.org/10.1175/1520-0442(1991)004<0957:ADARCC>2.0.CO;2

Numaguti, A. (1999). Origin and recycling processes of precipitating water over the Eurasian continent: Experiments using an atmospheric general circulation model. *Journal of Geophysical Research*, *104*(D2), 1957–1972. https://doi.org/10.1029/1998JD200026

Pierrehumbert, R. T. (1999). Huascaran δ18Oas an indicator of tropical climate during the Last Glacial Maximum. *Geophysical Research Letters*, *26*(9), 1345–1348. https://doi.org/10.1029/1999GL900183

Pope, V. D., Gallani, M. L., Rowntree, P. R., & Stratton, R. A. (2000). The impact of new physical parametrizations in the Hadley Centre climate model: HadAM3. *Climate Dynamics*, *16*(2-3), 123–146. https://doi.org/10.1007/s003820050009

Rayner, N. A., Parker, D. E., Horton, E. B., Folland, C. K., Alexander, L. V., Rowell, D. P., et al. (2003). Global analyses of sea surface temperature, sea ice, and night marine air temperature since the late nineteenth century. *Journal of Geophysical Research*, *108*(D14), 4407. https://doi.org/10.1029/2002JD002670

Reboita, M. S., da Rocha, R. P., Dias, C. G., & Ynoue, R. Y. (2014). Climate projections for South America: RegCM3 Driven by HadCM3 and ECHAM5. *Advances in Meteorology*, *2014*, 376738. https://doi.org/10.1155/2014/376738

Risi, C., Bony, S., Vimeux, F., Frankenberg, C., Noone, D., & Worden, J. (2010). Understanding the Sahelian water budget through the isotopic composition of water vapor and precipitation. *Journal of Geophysical Research*, *115*, D24110. https://doi.org/10.1029/2010JD014690

Risi, C., Noone, D., Frankenberg, C., & Worden, J. (2013). Role of continental recycling in intraseasonal variations of continental moisture as deduced from model simulations and water vapor isotopic measurements. *Water Resources Research*, *49*, 4136–4156. https://doi.org/10.1002/wrcr.20312

Risi, C., Ogée, J., Bony, S., Bariac, T., Raz-Yaseef, N., Wingate, L., et al. (2016). The water isotopic version of the land-surface model ORCHIDEE: Implementation, evaluation, sensitivity to hydrological parameters. *Hydrology: Current Research*, *07*, 258. https://doi.org/10.4172/2157-7587.1000258

Salati, E., Dall'Olio, A., Matsui, E., & Gat, J. R. (1979). Recycling of water in the Amazon Basin: An isotopic study. *Water Resources Research*, *15*(5), 1250–1258. https://doi.org/10.1029/WR015i005p01250

Schlesinger, W. H., & Jasechko, S. (2014). Transpiration in the global water cycle. *Agricultural and Forest Meteorology*, *189-190*, 115–117. https://doi.org/10.1016/j.agrformet.2014.01.011

Shukla, J., Nobre, C., & Sellers, P. (1990). Amazon deforestation and climate change. *Science*, *247*(4948), 1322–1325. https://doi.org/10.1126/science.247.4948.1322

Sime, L. C., Tindall, J. C., Wolff, E. W., Connolley, W. M., & Valdes, P. J. (2008). Antarctic isotopic thermometer during a CO2forced warming event. *Journal of Geophysical Research*, *113*, D24119. https://doi.org/10.1029/2008JD010395

Spera, S. A., Galford, G. L., Coe, M. T., Macedo, M. N., & Mustard, J. F. (2016). Land-use change affects water recycling in Brazil's last agricultural frontier. *Global Change Biology*, *22*(10), 3405–3413. https://doi.org/10.1111/gcb.13298

Staal, A., Tuinenburg, O. A., Bosmans, J. H. C., Holmgren, M., van Nes, E. H., Scheffer, M., et al. (2018). Forest-rainfall cascades buffer against drought across the Amazon. *Nature Climate Change*, *8*(6), 539–543. https://doi.org/10.1038/s41558-018-0177-y

Thompson, L. G., Mosley-Thompson, E., Davis, M. E., Lin, P. N., Henderson, K. A., Cole-Dai, J., et al. (1995). Late glacial stage and holocene tropical ice core records from huascaran, peru. *Science*, *269*(5220), 46–50. https://doi.org/10.1126/science.269.5220.46

Thompson, L. G., Mosley-Thompson, E., & Henderson, K. A. (2000). Ice-core palaeoclimate records in tropical South America since the Last Glacial Maximum. *Journal of Quaternary Science*, *15*(4), 377–394. https://doi.org/10.1002/1099-1417(200005)15:4<377::AID-JQS542>3.0.CO;2-L

Tindall, J. C., Valdes, P. J., & Sime, L. C. (2009). Stable water isotopes in HadCM3: Isotopic signature of El Nino Southern Oscillation and the tropical amount effect. *Journal of Geophysical Research*, *114*, D04111. https://doi.org/10.1029/2008JD010825

van Breukelen, M. R., Vonhof, H. B., Hellstrom, J. C., Wester, W. C. G., & Kroon, D. (2008). Fossil dripwater in stalagmites reveals Holocene temperature and rainfall variation in Amazonia. *Earth and Planetary Science Letters*, *275*(1-2), 54–60. https://doi.org/10.1016/j.epsl.2008.07.060

van der Ent, R. J., Savenije, H. H. G., Schaefli, B., & Steele-Dunne, S. C. (2010). Origin and fate of atmospheric moisture over continents. *Water Resources Research*, *46*, W09525. https://doi.org/10.1029/2010WR009127

Wang, X., Edwards, R. L., Auler, A. S., Cheng, H., Kong, X., Wang, Y., et al. (2017). Hydroclimate changes across the Amazon lowlands over the past 45,000 years. *Nature*, *541*(7636), 204–207. https://doi.org/10.1038/nature20787

Washburn, E. W., & Smith, E. R. (1934). The isotopic fractionation of water by physiological processes. *Science*, *79*(2043), 188–189. https://doi.org/10.1126/science.79.2043.188

Wright, J. S., Fu, R., Worden, J. R., Chakraborty, S., Clinton, N. E., Risi, C., et al. (2017). Rainforest-initiated wet season onset over the southern Amazon. *Proceedings of the National Academy of Sciences of the United States of America*, *114*(32), 8481–8486. https://doi.org/10.1073/pnas.1621516114

Yoshimura, K., Oki, T., Ohte, N., & Kanae, S. (2004). Colored moisture analysis estimates of variations in 1998 Asian monsoon water sources. *Journal of the Meteorological Society of Japan*, *82*(5), 1315–1329. https://doi.org/10.2151/jmsj.2004.1315

Zemp, D. C., Schleussner, C. F., Barbosa, H. M., Hirota, M., Montade, V., Sampaio, G., et al. (2017). Self-amplified Amazon forest loss due to vegetation-atmosphere feedbacks. *Nature Communications*, *8*(1), 14681. https://doi.org/10.1038/ncomms14681

Zhang, L., Dawes, W. R., & Walker, G. R. (2001). Response of mean annual evapotranspiration to vegetation changes at catchment scale. *Water Resources Research*, *37*(3), 701–708. https://doi.org/10.1029/2000WR900325